

Recounting the FANTOM Cage Associated Transcriptome

Eddie-Luidy Imada^{1,2,+}, Diego Fernando Sanchez^{1,+}, Leonardo Collado-Torres³, Christopher Wilks⁴, Tejasvi Matam¹, Wikum Dinalankara¹, Aleksey Stupnikov¹, Francisco Lobo-Pereira⁵, Chi-Wai Yip⁶, Kayoko Yasuzawa⁶, Naoto Kondo⁶, Masayoshi Itoh⁷, Harukazu Suzuki⁶, Takeya Kasukawa⁶, Chung Chau Hon⁶, Michiel de Hoon⁶, Jay W Shin⁶, Piero Carninci⁶, FANTOM consortium, Andrew E Jaffe^{3,8,9}, Jeffrey T Leek⁹, Alexander Favorov^{1,10}, Gloria R Franco², Ben Langmead^{4,9,*}, and Luigi Marchionni^{1,*,+,a}

¹Department of Oncology, Johns Hopkins University School of Medicine, Baltimore, MD, USA

²Departamento de Bioquímica e Imunologia, ICB, Universidade Federal de Minas Gerais, Belo Horizonte, MG, Brazil

³Lieber Institute for Brain Development, Baltimore, MD, USA

⁴Department of Computer Science, Johns Hopkins University, Baltimore, MD, USA

⁵Departamento de Biologia Geral, ICB, Universidade Federal de Minas Gerais, Belo Horizonte, MG, Brazil

⁶RIKEN Center for Integrative Medical Sciences, Yokohama, Japan

⁷RIKEN, Preventive Medicine Diagnostic Innovation Program, Yokohama, Japan

⁸Department of Mental Health, Johns Hopkins Bloomberg School of Public Health, Baltimore, MD, USA

⁹Department of Biostatistics, Johns Hopkins Bloomberg School of Public Health, Baltimore, MD, USA

¹⁰Laboratory of Systems Biology and Computational Genetics, VIGG RAS, Moscow, RF

^{*,+}These authors contributed equally to this work

^aCorrespondence to Luigi Marchionni (marchion@jhu.edu)

ABSTRACT

Long non-coding RNAs (lncRNAs) have emerged as key coordinators of biological and cellular processes. Characterizing lncRNA expression across cells and tissues is key to understanding their role in determining phenotypes including disease. We present here *FC-R2*, a comprehensive expression atlas across a broadly-defined human transcriptome, inclusive of over 100,000 coding and non-coding genes as described by the FANTOM CAGE-Associated Transcriptome (FANTOM-CAT) study. This atlas greatly extends the gene annotation used in the original *recount2* resource. We demonstrate the utility of the *FC-R2* atlas by reproducing key findings from published large studies and by generating new results across normal and diseased human samples. In particular, we (a) identify tissue specific transcription profiles for distinct classes of coding and non-coding genes, (b) perform differential expression analysis across thirteen cancer types, providing new insights linking promoter and enhancer lncRNAs expression to tumor pathogenesis, and (c) confirm the prognostic value of several enhancers in cancer. Comprised of over 70,000 samples, *FC-R2* will empower other researchers to investigate the roles of both known genes and recently described lncRNAs. Access to the *FC-R2* atlas is available from <https://jhubiostatistics.shinyapps.io/recount/>, the *recount* Bioconductor package, and <http://marchionnilab.org/fcr2.html>.

Introduction

Long non-coding RNAs (lncRNAs) are commonly defined as transcripts devoid of open reading frames (ORFs) longer than 200 nucleotides, which are often polyadenylated. This definition is not based on their function, since lncRNAs are involved in distinct molecular processes and biological contexts not yet fully characterized¹. Over the past few years, the importance of lncRNAs has been clarified, leading to an increasing focus on decoding the consequences of their modulation and studying their involvement in the regulation of key biological mechanisms during development, normal tissue and cellular homeostasis, and in disease¹⁻³.

Given the emerging and previously underestimated importance of non-coding RNAs, the FANTOM consortium has initiated the systematic characterization of their biological function. Through the use of Cap Analysis of Gene Expression sequencing (CAGE-seq), combined with RNA-seq data from the public domain, the FANTOM consortium released a comprehensive atlas of the human transcriptome, encompassing more accurate transcriptional start sites (TSS) for coding and non-coding genes, including numerous novel long non-coding genes: the FANTOM CAGE Associated Transcriptome (*FANTOM-CAT*)⁴. We hypothesized that these lncRNAs can be measured in many RNA-seq datasets from the public domain and that they have been so far missed by the lack of a comprehensive gene annotation.

Although the systematic analysis of lncRNAs function is being addressed by the FANTOM consortium in loss of function studies, increasing the detection rate of these transcripts combining different studies is difficult because the heterogeneity of analytic methods employed. Current resources that apply uniform analytic methods to create expression summaries from public data do exist but can miss several lncRNAs because their dependency on a pre-existing gene annotation for creating the genes expression summaries^{5,6}. We recently created *recount2*⁷, a collection of uniformly-processed human RNA-seq data, wherein we summarized 4.4 trillion reads from over 70,000 human samples from the Sequence Reads Archive (SRA), The Cancer Genome Atlas (TCGA)⁸, and the Genotype-Tissue Expression (GTEx)⁹ projects⁷. Importantly, *recount2* provides annotation-agnostic coverage files that allow re-quantification using a new annotation without having to re-process the RNA-seq data.

Given the unique opportunity to access latest results to the most comprehensive human transcriptome (the *FANTOM-CAT* project) and the *recount2* gene agnostic summaries, we addressed the previous described challenges building a comprehensive atlas of coding and non-coding gene expression across the human genome: the *FANTOM-CAT/recount2* expression atlas (FC-R2 hereafter). Our resource contains expression profiles for 109,873 putative genes across over 70,000 samples, enabling an unparalleled resource for the analysis of the human coding and non-coding transcriptome.

Results

Building the *FANTOM-CAT/recount2* resource

The *recount2* resource includes a coverage track, in the form of a BigWig file, for each processed sample. We built the FC-R2 expression atlas by extracting expression levels from *recount2* coverage tracks in regions that overlapped unambiguous

exon coordinates for the permissive set of *FANTOM-CAT* transcripts, according to the pipeline shown in Figure 1. Since *recount2*'s coverage tracks does not distinguish from between genomic strands, we removed ambiguous segments that presented overlapping exon annotations from both strands (see Methods section). After such disambiguation procedure, the remaining 1,066,515 exonic segments mapped back to 109,869 genes in *FANTOM-CAT* (out of the 124,047 starting ones included in the permissive set⁴). Overall, the FC-R2 expression atlas encompasses 2,041 studies with 71,045 RNA-seq samples, providing expression information for 22,116 coding genes and 87,763 non-coding genes, such as enhancers, promoters, and others lncRNAs.

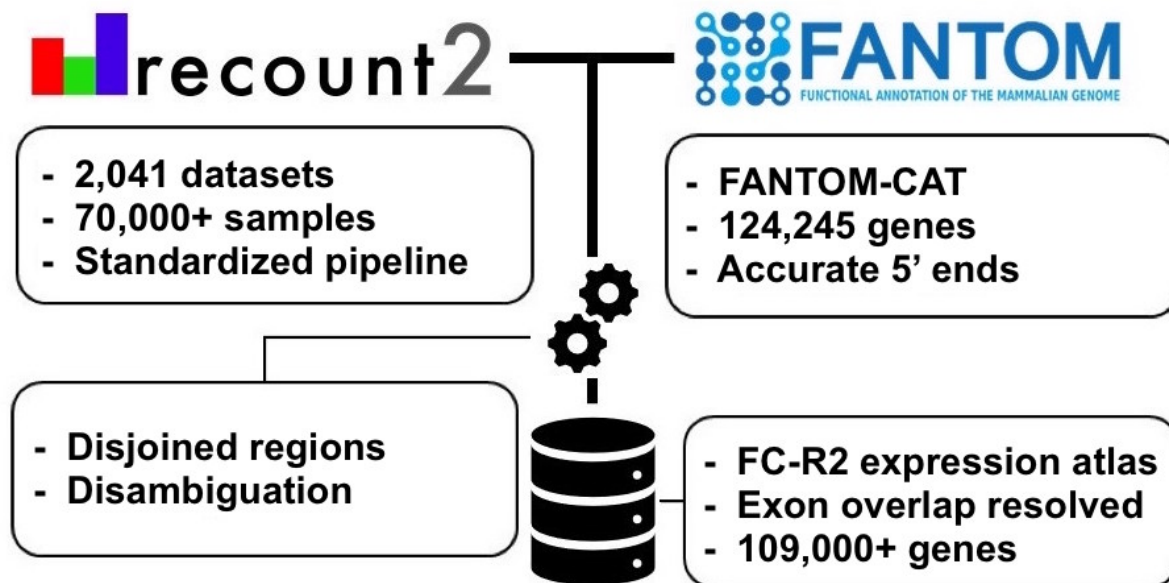


Figure 1. Overview of the *FANTOM-CAT/recount2* resource development. FC-R2 leverages two public resources, the *FANTOM-CAT* gene models and *recount2*. FC-R2 provides expression information for 109,873 genes, both coding (22,110) and non-coding (87,693). This latter group encompasses enhancers, promoters, and others lncRNAs.

Validating the *FANTOM-CAT/recount2* resource

We first assessed how gene expression estimates in FC-R2 compared to previous gene expression estimates from other projects. Specifically, we considered data from the GTEx consortium (v6), spanning 9,662 samples from 551 individuals and 54 tissues types⁹. First, we correlated gene expression levels between the FC-R2 atlas and quantification based on GENCODE (v25) in *recount2* for the GTEx data, observing a median correlation ≥ 0.986 for the 32,922 genes in common. This result supports the notion that our pre-processing steps to disambiguate overlapping exon regions between strands did not significantly alter gene expression quantification.

Next, we assessed whether gene expression specificity, as measured in FC-R2, was maintained across tissue types. To this end, we selected and compared gene expression for known tissue-specific expression patterns, such as Keratin 1 (*KRT1*), Estrogen Receptor 1 (*ESR1*), and Neuronal Differentiation 1 (*NEUROD1*) (Figure 2). Overall, all analyzed tissue specific markers presented nearly identical expression profiles across GTEx tissue types between the alternative gene models considered

(see Figure 2 and S1), confirming the consistency between gene expression quantification in FC-R2 and those based on GENCODE.

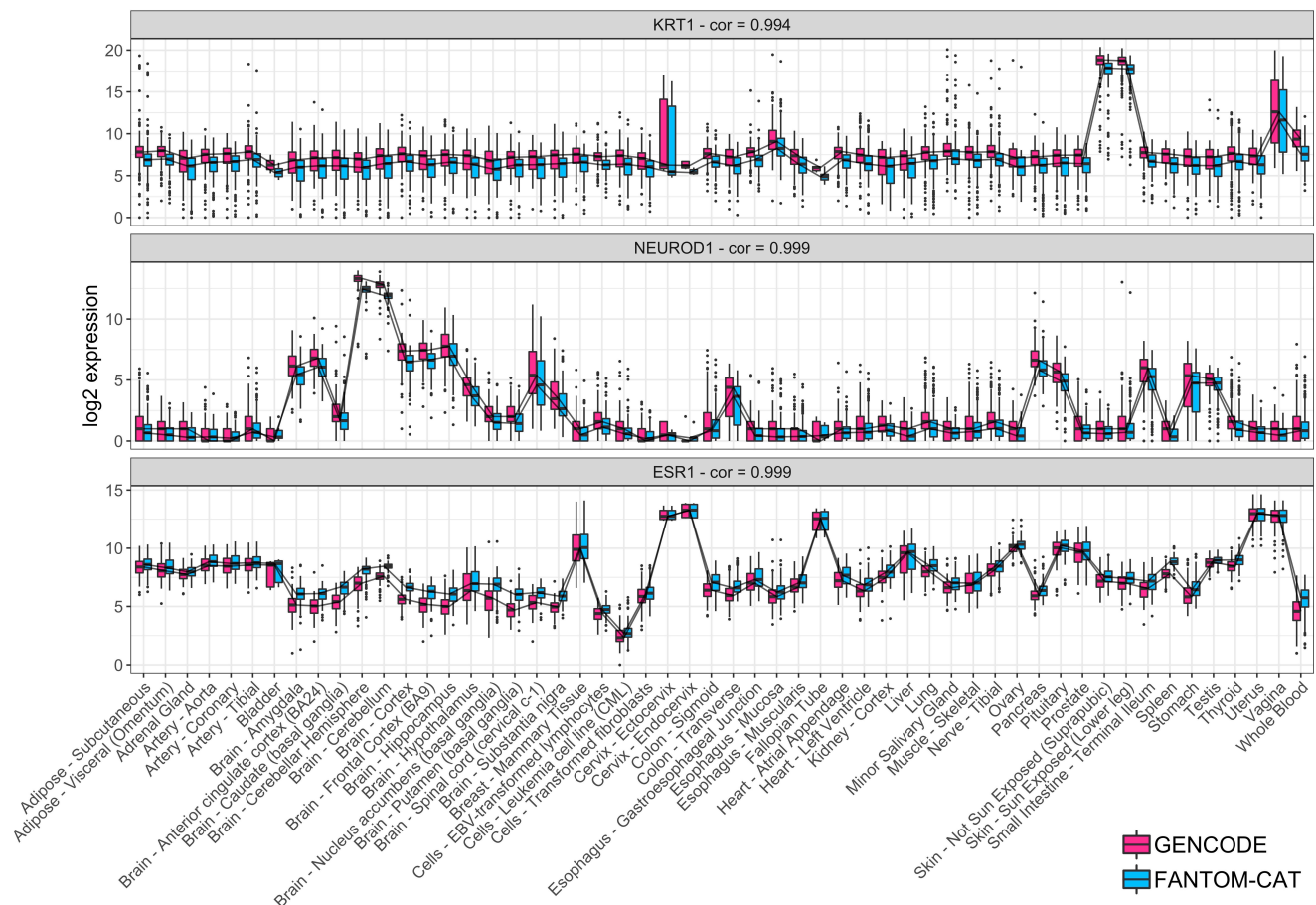


Figure 2. Tissue specific expression in GTEx. Log₂ expression for three tissue specific genes (*KRT1*, *NEUROD1*, and *ESR1*) in GTEx data stratify by tissue type using FC-R2 and GENCODE based quantification. Expression profiles are highly correlated and expressed consistently in the expected tissue types (e.g., *KRT1* is most expressed in skin, *NEUROD1* in brain, and *ESR1* in estrogen sensitive tissue types like uterus, Fallopian tubes, and breast). Correlations are shown on top for each tissue marker. Center lines, upper/lower quartiles and Whiskers represents the median, 25/75 quartiles and 1.5 interquartile range, respectively.

Tissue-specific expression of lncRNAs

It has been shown that, although expressed at a lower level, enhancers and promoters are not ubiquitously expressed and are more specific for different cell types than coding genes⁴. In order to verify this finding, we used GTEx data to assess expression levels and specificity profiles across samples from each of the 54 analyzed tissue types, stratified into four distinct gene categories: coding mRNA, intergenic promoter lncRNA (ip-lncRNA), divergent promoter lncRNA (dp-lncRNA), and enhancers lncRNA (e-lncRNA). Overall, we were able to confirm that these RNA classes are expressed at different levels, and that they display distinct specificity patterns across tissues, as shown for primary cell types by Hon et al.⁴, albeit with more variability likely due to the increased cellular complexity present in tissues. Specifically, coding mRNAs were expressed at higher levels

than lncRNAs (log2 median expression of 6.6 for coding mRNAs, and of 4.1, 3.8 and 3.1, for ip-lncRNA, dp-lncRNA, and e-lncRNA, respectively). In contrast, the expression of enhancers and intergenic promoters was more tissue-specific (median = 0.41 and 0.30) than what observed for divergent promoters and coding mRNAs (median = 0.13 and 0.09) (Figure 3). Finally, when analyzing the percentage of genes expressed across tissues by category, we observed that coding genes are, in general, ubiquitous, while lncRNAs are more specific, with enhancers showing the lowest percentages of expressed (mean ranging from 88.42% to 41.98%, see Figure 3B), in agreement with the notion that enhancer transcription is tissue specific¹⁰.

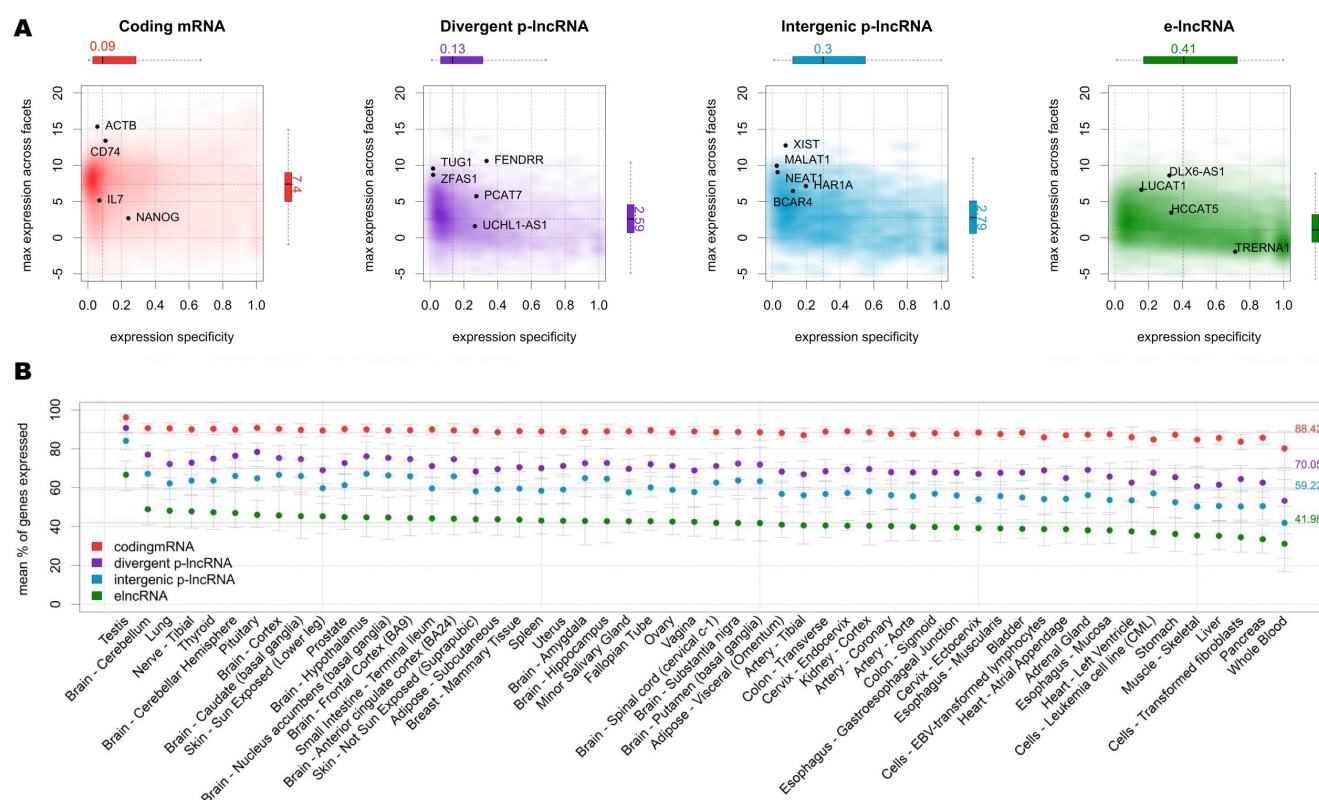


Figure 3. Expression profiles across GTEx tissues. **A)** Expression level and tissue specificity across four distinct RNA categories. The Y-axis shows log2 expression levels representing each gene using its maximum expression in GTEx tissues expressed as transcripts per million (TMP). The X-axis shows expression specificity based on entropy computed from median expression of each gene across the GTEx tissue types. Individual genes are highlighted in the figure panels. **B)** Percentage of genes expressed for each RNA category stratified by GTEx tissue facets. The dots represent the mean among samples within a facet and the error bars represent 99.99% confidence intervals. Dashed lines represent the means among all samples.

Differential expression analysis of coding and non-coding genes in cancer

We analyzed coding and non-coding gene expression in cancer using TCGA data. To this end, we compared cancer to normal samples separately for 13 tumor types, using FC-R2 re-quantified data. We further identified the differentially expressed genes (DEG) in common across the distinct cancer types (see Figure 4). Overall, the number of DEG varied across cancer types and by gene class, with a higher number of significant coding than non-coding genes (FDR < 0.01, see table 1). Importantly, a substantial fraction of these genes was exclusively annotated in the *FANTOM-CAT*, suggesting that relying on other gene

models would result in missing many potential important genes (see Table 1). We then analyzed the consensus among cancer types. A total of 41 coding mRNAs were differentially expressed across all the 13 tumor types after global correction for multiple testing ($FDR < 10^{-6}$, see Supplementary table S1). For lncRNAs, a total of 28 divergent promoters, 4 intergenic promoters, and 3 enhancers were consistently up- or down-regulated across all the 13 tumor types after global correction for multiple testing ($FDR < 0.1$, see Supplementary tables S2, S3, S4, respectively).

Table 1. Differentially expressed genes in cancer. The table below summarizes the number of significant DEG ($FDR \leq 0.01$) between tumor and normal samples across the 13 cancer types analyzed for each gene class considered (coding mRNA, ip-lncRNA, dp-lncRNA, and e-lncRNA). Counts are reported separately for DEG up- and down-regulated in cancer, and values in parenthesis represents the number of genes exclusively annotated in the *FANTOM-CAT* gene model. Mean and standard deviation across cancer types is shown at the bottom.

Cancer type	Total	dp-lncRNA		e-lncRNA		ip-lncRNA		mRNA	
		Up	Down	Up	Down	Up	Down	Up	Down
Bile	7010	200 (60)	313 (90)	186 (89)	203 (99)	47 (12)	84 (17)	2658 (106)	3319 (97)
Bladder	7680	344 (125)	319 (87)	140 (68)	149 (67)	65 (19)	82 (7)	3112 (201)	3469 (61)
Breast	15290	753 (291)	721 (202)	656 (377)	583 (305)	207 (50)	178 (32)	6109 (296)	6083 (244)
Colorectal	13685	490 (164)	592 (168)	381 (203)	400 (196)	130 (32)	160 (28)	5538 (371)	5994 (132)
Esophagus	4883	87 (21)	193 (50)	90 (38)	184 (103)	40 (11)	48 (2)	1921 (83)	2320 (77)
Head and Neck	10517	442 (138)	401 (96)	267 (139)	251 (112)	100 (23)	109 (18)	4329 (256)	4618 (53)
Kidney	15697	734 (238)	820 (281)	535 (299)	486 (209)	203 (45)	200 (48)	6349 (525)	6370 (114)
Liver	10554	346 (94)	395 (106)	230 (102)	248 (123)	90 (16)	112 (19)	4164 (174)	4969 (95)
Lung	17143	864 (338)	835 (304)	893 (512)	729 (396)	242 (76)	213 (39)	7523 (532)	5844 (212)
Prostate	13183	686 (287)	654 (218)	418 (254)	452 (214)	175 (55)	167 (30)	5153 (489)	5478 (128)
Stomach	11309	528 (213)	518 (164)	462 (291)	436 (240)	144 (51)	129 (22)	4509 (558)	4583 (89)
Thyroid	14264	752 (284)	804 (318)	527 (295)	594 (332)	161 (39)	174 (47)	5403 (189)	5849 (308)
Uterus	12906	641 (285)	713 (235)	454 (263)	612 (341)	210 (79)	225 (54)	5135 (335)	4916 (181)
Mean	11855	528 (195)	560 (178)	403 (225)	410 (211)	140 (39)	145 (28)	4762 (317)	4909 (138)
St. Dev	3650	237 (102)	218 (89)	225 (137)	189 (107)	67 (23)	55 (16)	1557 (167)	1234 (77)

Next, we reviewed the literature to assess functional correlates for these consensus genes. Most of the consensus up-regulated coding genes (Supplementary Table S1) participate in cell cycle regulation, cell division, DNA replication and repair, and chromosome segregation, and mitotic spindle checkpoints. Most of the consensus down-regulated mRNAs (Supplementary Table S1) are associated with metabolism and oxidative stress, transcriptional regulation, cell migration and adhesion, and with modulation of DNA damage repair and apoptosis.

Down-regulated dp-lncRNAs were mostly those associated with immune cells (*e.g.*, natural killer cells, T cell, and mature B-cells). Three genes, *RP11-276H19*, *RPL34-AS1*, and *RAP2C-AS1*, were reported to be implicated in cancer (Supplementary Table S2). The first controls epithelial-mesenchymal transition, the second is associated with tumor size increase, and the

third is associated with urothelial cancer after kidney cancer transplantation¹¹⁻¹³. Among up-regulated dp-lncRNA, *SNHG1* (Supplementary Table S2) was implicated in cellular proliferation, migration, invasion of different cancer types, and strongly up-regulated in osteosarcoma, non-small lung cancer, and gastric cancer^{14,15}.

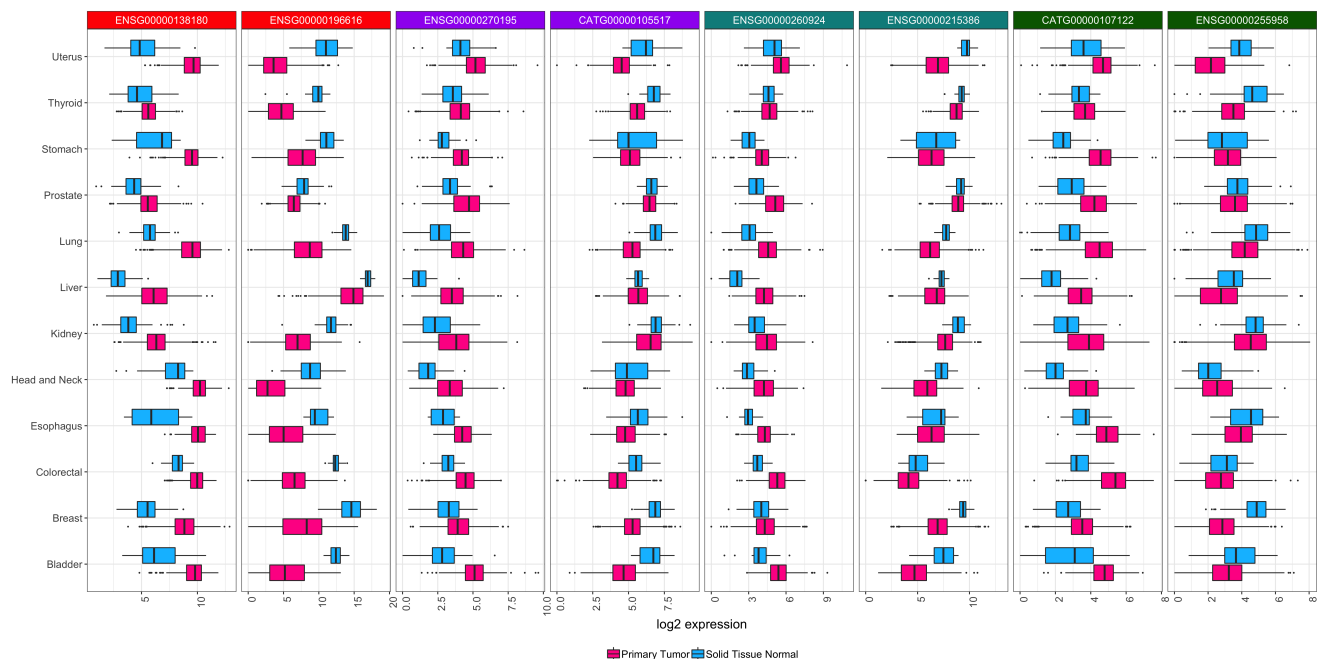


Figure 4. Differential expression for selected transcripts from distinct RNA classes across tumor types. Boxplots showing raw expression levels of differential expressed genes between tumor and normal tissue samples for all 13 tumor types analyzed. For each tissue of origin, the most up-regulated (on the left) and down-regulated (on the right) gene for each RNA class is shown. Center lines, upper/lower quartiles and Whiskers represents the median, 25/75 quartiles and 1.5 interquartile range, respectively. Color coding on top of the figure indicates the RNA class (red for mRNA, purple for dp-lncRNA, cyan ip-lncRNA, and green for e-lncRNA). These genes were select after global multiple testing correction (see Supplementary Tables S1, S2, S3, and S4)

Among the ubiquitously down-regulated ip-lncRNAs (see Supplementary Table S3), *LINC00478* has been previously reported in many different tumors including leukemia, breast, vulvar, prostate, and bladder cancer¹⁶⁻²⁰. In vulvar squamous cell carcinoma, there is a statistical relationship between *LINC00478* and *MIR31HG* expression and tumor differentiation¹⁷. Additionally, *LINC00478* down-regulated in ER positive breast tumors was shown to be associated with progression, recurrence, and metastasis¹⁸. In contrast, increased expression of *SNHG17* (an ip-lncRNA, see Supplementary Table S3), was associated with short term survival in breast cancer, and with tumor size, stage, and lymph node metastasis in colorectal cancer^{21,22}. Another ip-lncRNA, *AC004463*, (Supplementary Table S3), was found up-regulated in liver cancer and metastatic prostate cancer²³. Regarding the last lncRNA category considered here, we could not find any cancer association for common e-lncRNAs, nevertheless one, *RP5-965F6*, was previously reported to be up-regulated in late-onset Alzheimer's disease²⁴. The e-lncRNAs category also yielded the lowest number of genes in common among all cancer types, reinforcing the concept that lncRNAs, specially enhancers are expressed in a specific manner (Supplementary Table S4).

Finally, as a prototypical example, we considered prostate cancer (PCa), and we were able to confirm findings from previous

reports for both coding and non-coding genes (see Supplementary Figure S2). For coding genes, we confirmed differential expression for known markers of PCa progression and mortality, like *ERG*, *FOXA1*, *RNASEL*, *ARVCF*, and *SLC43A1*^{25,26}. Similarly, we also confirmed differential expression for non-coding genes, like *PCA3*, the first clinically approved lncRNA marker for PCa^{27,28}, *PCAT1*, a prostate-specific lncRNA involved in disease progression²⁹, *MALAT1*, which is associated with PCa poor prognosis³⁰, *CDKN2B-AS1*, an anti-sense lncRNA up-regulated in PCa that inhibits tumor suppressor genes activity^{31,32}, and the *MIR135* host gene, which is associated with castration-resistant PCa³³.

Enhancer expression levels hold prognostic value

The number of lncRNAs involved in cancer development and progression is rapidly increasing, we therefore analyzed the prognostic value of the lncRNAs we identified in our gene expression differential analysis in TCGA, as well as those previously reported in other studies. To this end, Chen and collaborators have recently surveyed enhancers expression in nearly 9,000 patients from the TCGA³⁴, using genomic coordinates from the FANTOM5 project³⁵, identifying 4,803 enhancers with prognostic potential in one or more tumor types in the TCGA. We therefore leveraged the FC-R2 atlas to identify prognostic coding and non-coding genes using Univariate Cox proportional hazard models, comparing our results for e-lncRNAs with those reported by Chen and colleagues.

When we considered e-lncRNA expression levels, we identified a total of 5,382 prognostic e-lncRNAs ($FDR \leq 0.05$), and no single one was predictive across all cancer types. Overall, the number of significant prognostic e-lncRNAs varied across tumors, ranging from 3 in head and neck cancer to 3,850 in kidney cancers (see Supplementary Table S6). Notably, two (out of three) e-lncRNAs from our differential gene expression consensus list across all tumor types were also prognostic. Specifically, *CATG00000107122* was associated with worst prognosis in kidney cancer, while *ENSG00000255958* was associated with worse survival in stomach tumor. Overall, despite differences in annotation and quantification (see Supplementary Table S5), we were able to confirm prognostic value for 2,765 e-lncRNAs out of the 4,803 reported by Chen et al³⁴, including “enhancer 22” (*ENSG00000272666*, which was highlighted as a promising prognostic marker for kidney cancer (Supplementary Figure S3).

Finally, we analyzed the prognostic value for dp-lncRNAs, ip-lncRNAs, and mRNAs (See Supplementary Tables S7, S8, and S9, respectively), and assessed the survival prognostic potential of our consensus genes across tumor types. Thirty-seven of the 41 coding mRNAs, 22 of the 28 differentially expressed dp-lncRNAs, and two out of the four DE ip-lncRNAs, respectively, were found to be prognostic (See Supplementary Tables S10, S11, S12, and S13). Kaplan-Meier survival curves for one selected DE gene on each RNA subtype evaluated here are shown in supplementary figure S4.

Discussion

The importance of lncRNAs in cell biology and disease has clearly emerged in the past few years and different classes of lncRNAs have been shown to play crucial roles in cell regulation and homeostasis³⁶. For instance, enhancers – a major category of gene regulatory elements, which has been shown to be expressed^{35,37} – play a prominent role in oncogenic processes^{38,39}

and other human diseases^{40,41}. Despite their importance, however, there is a scarcity of large-scale datasets investigating enhancers and other lncRNA classes, in part due to the technical difficulty in applying high-throughput techniques such as ChIP-seq and Hi-C over large cohorts, and to the use of gene models that do not account for them in transcriptomics analyses. Furthermore, the large majority of the lncRNAs that are already known – and that have been shown to be associated with some phenotype – are still lacking functional annotation.

To address these needs, the FANTOM consortium has first constructed the *FANTOM-CAT* meta-transcriptome, a comprehensive atlas of coding and non-coding genes with robust support from CAGE-seq data⁴, then it has undertaken a large scale project to systematically target lncRNAs and characterize their function using a multi-pronged approach (Jordan et al., under review). In a complementary effort, we have leveraged public domain gene expression data from *recount2*^{7,42} to create a comprehensive gene expression compendium across human cells and tissues based on the *FANTOM-CAT* gene model, with the ultimate goal of facilitating lncRNAs annotation through association studies.

In order to validate our resource, we have compared the gene expression summaries based on *FANTOM-CAT* gene models with previous, well-established quantification of gene expression, demonstrating virtually identical profiles across tissue types overall and for specific tissue markers. We have then confirmed that distinct classes of coding and non-coding genes differ in terms of overall expression levels and specificity patterns across cell types and tissues. Furthermore, with this approach, we were also able to identify mRNAs, promoters, enhancers, and other lncRNAs that are differentially expressed in cancer, both confirming previously reported findings, and identifying novel cancer genes exclusively annotated in the *FANTOM-CAT* gene model, which have been therefore missed in prior analyses with TCGA data. Finally, we also analyzed the prognostic value of the coding and non-coding genes we identified in our analyses, and confirmed the association with overall survival in TCGA for measurable enhancers.

Collectively, by confirming findings reported in previous studies, our results demonstrate that the FC-R2 gene expression atlas is a reliable and powerful resource for exploring both the coding and non-coding transcriptome, providing compelling evidence and robust support to the notion that lncRNA gene classes, including enhancers and promoters, despite not being yet fully understood, portend significant biological functions. Our resource, therefore, constitutes a suitable and promising platform for future large scales studies in cancer and other human diseases, which in turn hold the potential to reveal important cues to the understanding of their biological, physiological, and pathological roles, potentially leading to improved diagnostic and therapeutic interventions.

Finally, all results and data from the FC-R2 atlas are available as a public tool. With uniformly processed expression data for over 70,000 samples and 109,873 genes ready to analyze, we want to encourage researchers to dive deeper into the study of ncRNAs, their interaction with coding and non-coding genes, and their influence on normal and disease tissues. We hope this new resource will help paving the way to develop new hypotheses that can be followed to unwind the biological role of the transcriptome as a whole.

Methods

Data and pre-processing.

FANTOM CAT permissive catalog was obtained from the pre-FANTOM6 consortium. This catalog initially comprised 124,245 genes defined by CAGE peaks published by Hon et al⁴. In order to remove ambiguity, BED files containing the coordinates for each gene/exon were imported into an R session and processed with the GenomicRanges package⁴³ by disjoining the exon coordinates. To avoid losing strand information we processed it in a two-step approach by first disjoining overlapping segments on the same strand and latter across strands (Figure 5). Genomic ranges (disjoined exons segments) that mapped back to more than one gene were discarded. The expression values for these ranges were then quantified using *recount.bwtool*⁴⁴ (code at https://github.com/LieberInstitute/marchionni_projects). The resulting expression quantifications were processed to generate `RangedSummarizedExperiment` objects compatible with the *recount2* framework^{7,42} (code at <https://github.com/eddieimada/fcr2>). Thus FC-R2 provides expression information for coding mRNAs, enhancers and promoters (divergent and intergenic) for 9,662 samples from the Genotype-Tissue Expression (GTEx) project, 11,350 samples from The Cancer Genome Atlas (TCGA) consortium, and over 50,000 samples from the Sequence Read Archive (SRA).

Correlation with other studies.

To test if the pre-processing step had a major impact on expression quantification, we compared our counts tables to the published GTEx counts from *recount2*. The version 2 of the gene counts for the GTEx samples were downloaded from the recount website (<https://jhubiostatistics.shinyapps.io/recount/>). We compared distribution of tissue specific genes across tissues and computed the Pearson correlation for each gene in common across the original *recount2* gene counts estimates and our version.

Expression specificity of tissue facets.

We analyzed the expression level and specificity of each gene stratified by RNA class (i.e. mRNA, e-lncRNA, dp-lncRNA, ip-lncRNA). Expression levels for each gene were represented by the maximum transcripts per million (TPM) of all samples within a facet. To compute the gene specificity we followed the same approach used in Hon et al⁴. The 99.99 percent confidence intervals for the expression of each category by facet were calculated based on TPM values. Genes with a TPM greater than 0.01 were considered expressed.

Identification of differentially expressed genes.

Differential gene expression was tested in 13 cancer types, comparing primary tumor with normal samples using TCGA FC-R2 gene expression summaries. Summaries for each cancer type were split by RNA class (coding mRNA, intergenic promoter lncRNA, divergent promoter lncRNA and enhancer lncRNA) and analyzed independently. A generalized linear model approach coupled with empirical Bayes standard errors⁴⁵ was used to identify differentially expressed genes between the samples. The

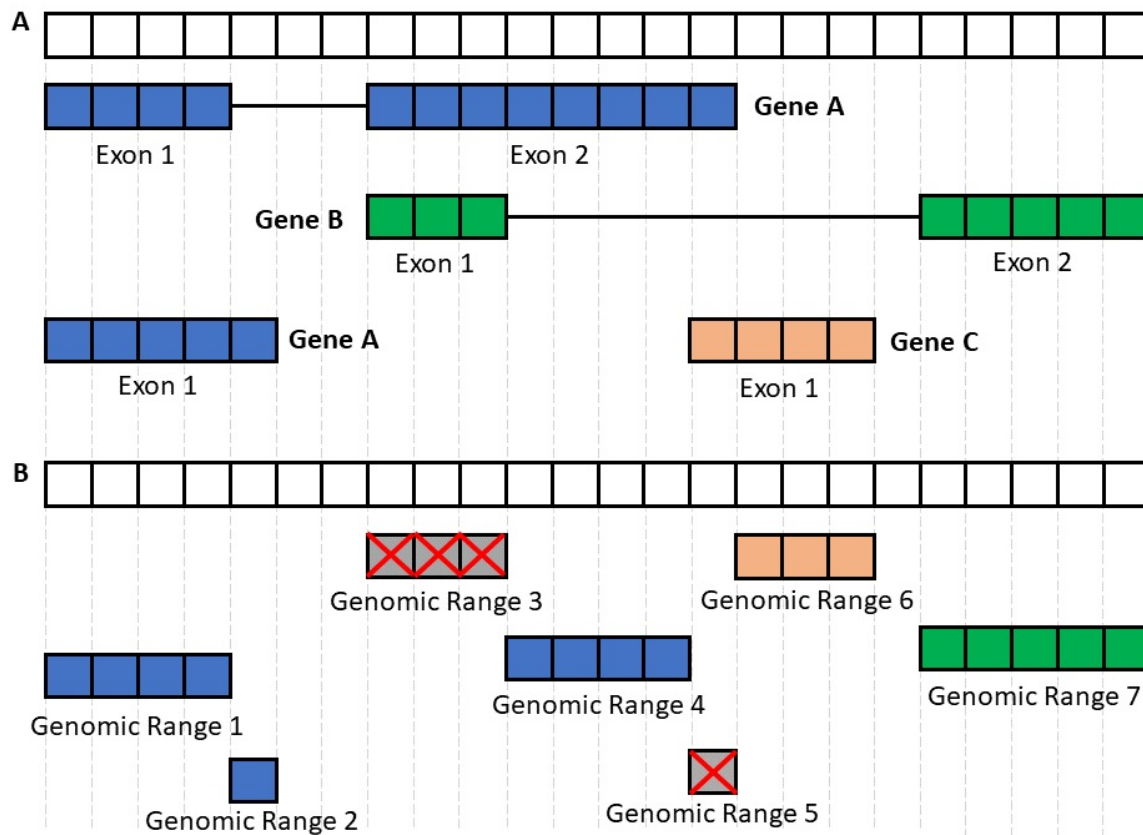


Figure 5. FANTOM-CAT genomic ranges. Representation of the disjoining and exon disambiguation processes. (A) Representation of a genome segment and its annotation containing 3 genes with gene A having two isoforms, and genes B and C with one isoform each. Each box can be interpreted as one nucleotide with boxes colored blue or orange to represent exons on opposite strands. (B) Representation of disjointed exon ranges from example A. Each feature is reduced to a set of non-overlapping genomic ranges, then genomic ranges mapping back to two or more genes are removed (crossed boxes). After removal of ambiguous ranges, the remaining ranges are summarized at gene level. Grey boxes represent segments with ambiguous strand.

model was adjusted for the three most variable coefficients for data heterogeneity as estimated by surrogate variable analysis (SVA)⁴⁶. Correction for multiple testing was performed across RNA classes by merging the resulting p-values for each cancer type and applying the Benjamini-Hochberg method⁴⁷.

Prognostic analysis.

To evaluate the prognostic potential of the genes in FC-R2 we applied a univariate Cox proportional regression model in four RNA classes (22106 mRNAs, 17,404 e-lncRNAs, 6,204 dp-lncRNAs, and 1,948 ip-lncRNAs) comprised in FC-R2 across each of the 13 TCGA cancer types with available survival follow-up. Genes with FDR equal or less than 0.05 using Benjamini-Hochberg⁴⁷ correction within the cancer type and RNA class, were selected as significant prognostic factors. To identify differentially expressed genes that portrait predictive potential, the DE lists were intersected with the significant prognostic genes lists. Supplementary data from Chen et al³⁴ containing enhancers position and prognostic potential were

obtained from the original publication and a liftover to hg38 genome assembly was performed to match FC-R2 coordinates in order to compare the results.

Data Availability

All data is available in <http://marchionnilab.org/fcr2.html>. Expression data can be directly accessed through <https://jhubiostatistics.shinyapps.io/recount/> and the *recount* Bioconductor package (v1.9.5 or newer) at <https://bioconductor.org/packages/recount> as *RangedSummarizedExperiment* objects organized by The Sequence Read Archive (SRA) study ID. The data can be loaded using R-programming language and is ready to be analyzed using Bioconductor packages or the data can be exported to other formats for use in another environment.

Code Availability

All code used in this manuscript is available in: <https://github.com/eddieimada/fcr2> and https://github.com/LieberInstitute/marchionni_projects for reproducibility purposes.

Acknowledgements

This publication was made possible through support from the NIH-NCI grants P30CA006973 (L.M. and A.F.) and R01CA200859 (W.D. and L.M.), NIH-NIGMS grant R01GM118568 (C.W. and B.L.), R21MH109956-01 (L.C.T. and A.E.J.), and the Department of Defense (DoD) office of the Congressionally Directed Medical Research Programs (CDMRP) award W81XWH-16-1-0739 (E.L.I. and L.M.), RFBR 17-00-00208 (A.F.) and Russian Academic project 0112-2019-0001 (A.F.), Fundação de Amparo à Pesquisa do Estado de Minas Gerais award BDS-00493-16 (E.L.I. and G.R.F.). *recount2* and FC-R2 are hosted on SciServer, a collaborative research environment for large-scale data-driven science. It is being developed at, and administered by, the Institute for Data Intensive Engineering and Science (IDIES) at Johns Hopkins University. SciServer is funded by the National Science Foundation Award ACI-1261715. For more information about SciServer, visit <http://www.sciserver.org/>.

Author contributions statement

L.M. conceived the idea, L.M., E.I., A.F. and B.L. designed the study; E.L.I., D.F.S., T.M., W.D., A.S., L.C.T., and L.M. performed the analysis; E.L.I., D.F.S., F.P.L., G.R.F. and L.M. interpreted the results; L.C.T., C.W., C.Y., K.Y., N.K., M.I., H.S., T.K., C.C.H., M.H., J.W.S., P.C. A.E.J., J.T.L. and B.L. provided the data and tools; E.L.I., D.F.S., L.C.T., B.L. and L.M. wrote the manuscript; All authors reviewed and approved the manuscript.

Disclosure declaration

All authors declare no conflicts of interest.

References

1. Batista, P. J. & Chang, H. Y. Long noncoding RNAs: cellular address codes in development and disease. *Cell* **152**, 1298–1307 (2013). URL <http://eutils.ncbi.nlm.nih.gov/entrez/eutils/elink.fcgi?dbfrom=pubmed&id=23498938&retmode=ref&cmd=prlinks>. DOI 10.1016/j.cell.2013.02.012.
2. Esteller, M. Non-coding RNAs in human disease. *Nat. reviews Genet.* **12**, 861–874 (2011). URL <https://www.nature.com/articles/nrg3074>. DOI 10.1038/nrg3074.
3. Ling, H. et al. Junk DNA and the long non-coding RNA twist in cancer genetics. *Oncogene* **34**, 5003–5011 (2015). URL <http://www.nature.com/articles/onc2014456>. DOI 10.1038/onc.2014.456.
4. Hon, C.-C. et al. An atlas of human long non-coding RNAs with accurate 5' ends. *Nat.* **543**, 199–204 (2017). URL <http://www.nature.com/doifinder/10.1038/nature21374>. DOI 10.1038/nature21374.
5. Lachmann, A. et al. Massive mining of publicly available RNA-seq data from human and mouse. *Nat Commun* **9**, 1366 (2018).
6. Tatlow, P. J. & Piccolo, S. R. A cloud-based workflow to quantify transcript-expression levels in public cancer compendia. *Sci Rep* **6**, 39259 (2016).
7. Collado-Torres, L. et al. Reproducible RNA-seq analysis using recount2. *Nat. Biotechnol.* **35**, 319–321 (2017). URL <http://www.nature.com/doifinder/10.1038/nbt.3838>. DOI 10.1038/nbt.3838.
8. Network, C. G. A. R. et al. The Cancer Genome Atlas Pan-Cancer analysis project. *Nat. Genet.* **45**, 1113–1120 (2013). URL <http://eutils.ncbi.nlm.nih.gov/entrez/eutils/elink.fcgi?dbfrom=pubmed&id=24071849&retmode=ref&cmd=prlinks>. DOI 10.1038/ng.2764.
9. GTEx Consortium. The Genotype-Tissue Expression (GTEx) project. *Nat. Genet.* **45**, 580–585 (2013). URL <http://www.nature.com/articles/ng.2653>. DOI 10.1038/ng.2653.
10. Ong, C.-T. & Corces, V. G. Enhancer function: new insights into the regulation of tissue-specific gene expression. *Nat. Rev. Genet.* **12**, 283 (2011).
11. Zhou, M. et al. Lncrna-hh strengthen cancer stem cells generation in twist-positive breast cancer via activation of hedgehog signaling pathway. *Stem cells* **34**, 55–66 (2016).
12. Zhao, J. et al. Long non-coding rna linc00152 is involved in cell cycle arrest, apoptosis, epithelial to mesenchymal transition, cell migration and invasion in gastric cancer. *Cell cycle* **14**, 3112–3123 (2015).
13. Shang, D., Zheng, T., Zhang, J., Tian, Y. & Liu, Y. Profiling of mrna and long non-coding rna of urothelial cancer in recipients after renal transplantation. *Tumor Biol.* **37**, 12673–12684 (2016).
14. Cao, W.-J., Wu, H.-L., He, B.-S., Zhang, Y.-S. & Zhang, Z.-Y. Analysis of long non-coding rna expression profiles in gastric cancer. *World journal gastroenterology: WJG* **19**, 3658 (2013).

15. Sun, Y. et al. The long noncoding rna snhg1 promotes tumor growth through regulating transcription of both local and distal genes. Oncogene **36**, 6774 EP – (2017). URL <https://doi.org/10.1038/onc.2017.286>.
16. Emmrich, S. et al. Lincnas monoc and mir100hg act as oncogenes in acute megakaryoblastic leukemia. Mol. cancer **13**, 1 (2014).
17. Ni, S., Zhao, X. & Ouyang, L. Long non-coding rna expression profile in vulvar squamous cell carcinoma and its clinical significance. Oncol. reports **36**, 2571–2578 (2016).
18. Gökmen-Polar, Y. et al. Abstract p2-06-05: Linc00478: A novel tumor suppressor in breast cancer (2016).
19. Sun, D. et al. Regulation of several androgen-induced genes through the repression of the mir-99a/let-7c/mir-125b-2 mirna cluster in prostate cancer cells. Oncogene **33**, 1448 (2014).
20. Li, S. et al. Exploring functions of long noncoding rnas across multiple cancers through co-expression network. Sci. reports **7**, 754 (2017).
21. Zhao, W., Luo, J. & Jiao, S. Comprehensive characterization of cancer subtype associated long non-coding rnas and their clinical implications. Sci. reports **4**, 6591 (2014).
22. Ma, Z. et al. Long non-coding rna snhg17 is an unfavourable prognostic factor and promotes cell proliferation by epigenetically silencing p57 in colorectal cancer. Mol. BioSystems **13**, 2350–2361 (2017).
23. Zhu, S. et al. Genome-scale deletion screening of human long non-coding rnas using a paired-guide rna crispr-cas9 library. Nat. biotechnology **34**, 1279 (2016).
24. Humphries, C. E. et al. Integrated whole transcriptome and dna methylation analysis identifies gene networks specific to late-onset alzheimer's disease. J. Alzheimer's Dis. **44**, 977–987 (2015).
25. Lin, D. W. et al. Genetic variants in the LEPR, CRY1, RNASEL, IL4, and ARVCF genes are prognostic markers of prostate cancer-specific mortality. Cancer Epidemiol Biomarkers Prev **20**, 1928–1936 (2011). URL <http://cebp.aacrjournals.org/content/20/9/1928.abstract>. DOI 10.1158/1055-9965.EPI-11-0236.
26. Yu, J. et al. An integrated network of androgen receptor, polycomb, and TMPRSS2-ERG gene fusions in prostate cancer progression. Cancer cell **17**, 443–454 (2010). URL http://www.sciencedirect.com/science?_ob=ArticleURL&_udi=B6WWK-503HV0F-7&_user=75682&_coverDate=05%2F18%2F2010&_rdoc=1&_fmt=high&_orig=gateway&_origin=gateway&_sort=d&_docanchor=&view=c&_acct=C000006078&_version=1&_urlVersion=0&_userid=75682&md5=1893cfe1116f128f58fa146786f4e208&searchtype=a. DOI 10.1016/j.ccr.2010.03.018.
27. Bussemakers, M. J. et al. DD3: a new prostate-specific gene, highly overexpressed in prostate cancer. Cancer Res. **59**, 5975–5979 (1999).

28. de Kok, J. B. et al. DD3(PCA3), a very sensitive and specific marker to detect prostate tumors. Cancer Res **62**, 2695–2698 (2002). URL <http://eutils.ncbi.nlm.nih.gov/entrez/eutils/elink.fcgi?dbfrom=pubmed&id=11980670&retmode=ref&cmd=prlinks>.
29. Prensner, J. R. et al. Transcriptome sequencing across a prostate cancer cohort identifies PCAT-1, an unannotated lincRNA implicated in disease progression. Nat. Biotechnol. **29**, 742–749 (2011). URL <http://www.nature.com/articles/nbt.1914>. DOI 10.1038/nbt.1914.
30. Ren, S. et al. Long noncoding RNA MALAT-1 is a new potential therapeutic target for castration resistant prostate cancer. The J. Urol. **190**, 2278–2287 (2013). URL <http://eutils.ncbi.nlm.nih.gov/entrez/eutils/elink.fcgi?dbfrom=pubmed&id=23845456&retmode=ref&cmd=prlinks>. DOI 10.1016/j.juro.2013.07.001.
31. Gutschner, T. & Diederichs, S. The hallmarks of cancer: a long non-coding RNA point of view. RNA Biol **9**, 703–719 (2012). URL <http://eutils.ncbi.nlm.nih.gov/entrez/eutils/elink.fcgi?dbfrom=pubmed&id=22664915&retmode=ref&cmd=prlinks>. DOI 10.4161/rna.20481.
32. Kotake, Y. et al. Long non-coding RNA ANRIL is required for the PRC2 recruitment to and silencing of p15(INK4B) tumor suppressor gene. Oncogene **30**, 1956–1962 (2011). URL <https://www.nature.com/articles/onc2010568>. DOI 10.1038/onc.2010.568.
33. Huang, X. et al. Exosomal miR-1290 and miR-375 as prognostic markers in castration-resistant prostate cancer. Eur. urology **67**, 33–41 (2015). URL <http://linkinghub.elsevier.com/retrieve/pii/S0302283814006873>. DOI 10.1016/j.eururo.2014.07.035.
34. Chen, H., Li, C., Peng, X., Zhou, Z., Weinstein, J. N., Liang, H. A promoter-level mammalian expression atlas. Cell **173**, 386–399 (2018).
35. Andersson, R. et al. An atlas of active enhancers across human cell types and tissues. Nat. **507**, 455–461 (2014). URL <http://eutils.ncbi.nlm.nih.gov/entrez/eutils/elink.fcgi?dbfrom=pubmed&id=24670763&retmode=ref&cmd=prlinks>. DOI 10.1038/nature12787.
36. Quinn, J. J. & Chang, H. Y. Unique features of long non-coding rna biogenesis and function. Nat. Rev. Genet. **17**, 47 (2016).
37. Arner, E. et al. Transcribed enhancers lead waves of coordinated transcription in transitioning mammalian cells. Sci. (New York, NY) (2015). URL <http://eutils.ncbi.nlm.nih.gov/entrez/eutils/elink.fcgi?dbfrom=pubmed&id=25678556&retmode=ref&cmd=prlinks>. DOI 10.1126/science.1259418.
38. Sur, I. & Taipale, J. The role of enhancers in cancer. Nat. Rev. Cancer **16**, 483 (2016).
39. Herz, H.-M., Hu, D. & Shilatifard, A. Enhancer malfunction in cancer. Mol. cell **53**, 859–866 (2014).
40. Blencowe, B. J. Exonic splicing enhancers: mechanism of action, diversity and role in human genetic diseases. Trends biochemical sciences **25**, 106–110 (2000).

41. Hnisz, D. et al. Super-enhancers in the control of cell identity and disease. Cell **155**, 934–947 (2013).
42. Collado-Torres, L., Nellore, A. & Jaffe, A. E. recount workflow: Accessing over 70,000 human RNA-seq samples with Bioconductor. F1000Research **6**, 1558 (2017). URL <https://f1000research.com/articles/6-1558/v1>. DOI 10.12688/f1000research.12223.1.
43. Lawrence, M. et al. Software for computing and annotating genomic ranges. PLoS Comput. Biol. **9**, e1003118 (2013). URL <http://eutils.ncbi.nlm.nih.gov/entrez/eutils/elink.fcgi?dbfrom=pubmed&id=23950696&retmode=ref&cmd=prlinks>. DOI 10.1371/journal.pcbi.1003118.
44. Ellis, S. E., Collado-Torres, L., Jaffe, A. & Leek, J. T. Improving the value of public RNA-seq expression data by phenotype prediction. Nucleic Acids Res. **46**, e54–e54 (2018). URL <https://doi.org/10.1093/nar/gky102>. DOI 10.1093/nar/gky102. <http://oup.prod.sis.lan/nar/article-pdf/46/9/e54/24829382/gky102.pdf>.
45. Smyth, G. K. Linear models and empirical bayes methods for assessing differential expression in microarray experiments. Stat. applications genetics molecular biology **3**, Article3 (2004). URL <http://www.ncbi.nlm.nih.gov/pubmed/16646809?dopt=abstract>. DOI 10.2202/1544-6115.1027.
46. Leek, J. T. & Storey, J. D. Capturing heterogeneity in gene expression studies by surrogate variable analysis. PLoS genetics **3**, 1724–1735 (2007). URL <http://www.plosgenetics.org/article/info%3Adoi%2F10.1371%2Fjournal.pgen.0030161>. DOI 10.1371/journal.pgen.0030161.
47. Benjamini, Y. & Hochberg, Y. Controlling the false discovery rate: a practical and powerful approach to multiple testing. J. Royal Stat. Soc. Series B, **57**, 289–300 (1995). URL http://www.dm.uba.ar/materias/analisis_expl_y_conf_de_datos_de_exp_de_marrays_Mae/2006/1/teoricas/FDR%201995.pdf.
48. Buja, A. & Eyuboglu, N. Remarks on parallel analysis. Multivar. behavioral research **27**, 509–540 (1992).
49. Therneau, T. M. A Package for Survival Analysis in S (2015). URL <https://CRAN.R-project.org/package=survival>. Version 2.38.
50. Kassambara, A. & Kosinski, M. survminer: Drawing Survival Curves using 'ggplot2' (2018). URL <https://CRAN.R-project.org/package=survminer>. R package version 0.4.3.